

LETTER OPEN



ACUTE LYMPHOBLASTIC LEUKEMIA

Unusual PDGFRB fusion reveals novel mechanism of kinase activation in Ph-like B-ALL

Teresa Sadras^{1,2,12}, Fatimah B. Jalud^{1,12}, Hansen J. Kosasih³, Christopher R. Horne^{4,5}, Lauren M. Brown^{6,7}, Sam El-Kamand⁸, Charles E. de Bock^{9,7}, Lachlan McAloney^{1,8}, Ashley P. Ng^{1,4,5}, Nadia M. Davidson^{4,5,9}, Louise E. A. Ludlow^{3,8}, Alicia Oshlack^{1,2,10}, Mark J. Cowley^{6,7}, Seong L. Khaw^{3,8,11}, James M. Murphy^{4,5} and Paul G. Ekert^{1,2,3,6,7}✉

© The Author(s) 2023

Leukemia (2023) 37:905–909; <https://doi.org/10.1038/s41375-023-01843-x>

TO THE EDITOR:

Philadelphia-like (Ph-like) B-cell precursor acute lymphoblastic leukemia (B-ALL) is a high-risk subtype of leukaemia [1]. It is characterized by a gene expression profile similar to Philadelphia chromosome positive (Ph⁺) ALL, but lacking the *BCR::ABL1* rearrangement. Instead, Ph-like B-ALL represents a heterogeneous subtype driven by a diverse range of genetic aberrations and chromosomal rearrangements that converge on activated tyrosine kinase signalling [2, 3]. Integration of tyrosine kinase inhibitors into treatment regimens of Ph-like ALL patients has demonstrated early evidence of therapeutic efficacy, although results from larger clinical trials are pending [4].

Here we describe a novel PDGFRB lesion in a pediatric patient with Ph-like B-ALL. Unlike other PDGFRB fusions, this *CD74::PDGFRB* variant does not form a chimeric protein, yet is constitutively active and sufficient to drive oncogenic transformation. We provide a model for a unique mechanism of kinase activation in Ph-like ALL which has implications for diagnostic fusion identification and provides key insights into kinase biology.

The patient, a 22-month-old girl, presented with B-ALL and 86% blasts in the bone marrow (BM). Microarray analysis of the BM sample showed losses of chromosome regions 5q32 (partial *PDGFRB* and *CD74*), 7p12.2 (46 kb, intragenic *IKZF1* including exons 4 to 7), and 9p13.3-p13.1 (5 Mb, including *PAX5*, sub-clonal ~70 %). The patient was stratified as high-risk and treated on the COG AALL1131 trial. At the end of induction, residual blasts of 46.3% were still detected. Given indications of a *PDGFRB* lesion, the patient received dasatinib in combination with consolidation chemotherapy, but despite a measurable response, maintained persistent minimal residual disease (0.396%) at the end of consolidation. The patient proceeded to receive a Kymriah CAR T infusion. Additional clinical details are provided in the Supplemental Materials section.

We performed RNA-sequencing on the diagnostic sample. Gene expression analysis identified a Ph-like signature [5], and

highlighted aberrant expression of *PDGFRB* (Supplementary Fig. 1a). Sequence analysis confirmed a ~240 kb interstitial deletion in chromosome 5, resulting in a fusion between *CD74* (exon 1) and *PDGFRB* (exon 11) (Fig. 1a). The fusion was validated by PCR amplification of the breakpoint (Supplementary Fig. 1b), and the full length *CD74::PDGFRB* cDNA was amplified and cloned into an MSCV-IRES-GFP (MIG) expression plasmid. Sanger sequencing revealed a retained 75 bp *CD74* intronic sequence resulting in a stop codon before the fusion junction (Fig. 1b). We henceforth refer to this novel fusion as *CD74^{intr}::PDGFRB*. A previous report described a *CD74::PDGFRB* variant resulting in an in-frame fusion linking *CD74* exon 6 and *PDGFRB* exon 11 [6]. However, our patient's fusion is distinguished by the absence of a clear open reading frame (ORF) to drive translation of an in-frame fusion protein. To determine whether a PDGFRB species is produced as a result of the *CD74^{intr}::PDGFRB* fusion, we used western blotting to analyze leukemic mononuclear (MNC) cells from the patient (Fig. 1c). Strikingly, an immunoreactive PDGFRB species of ~60 kDa was detected in the patient MNCs corresponding to an equivalent product detected in murine Ba/F3 cells engineered to express the *CD74^{intr}::PDGFRB* cDNA cloned directly from the patient.

To functionally characterize the novel *CD74^{intr}::PDGFRB* fusion, we stably transduced IL-3-dependent mouse pro-B Ba/F3 cells with *CD74^{intr}::PDGFRB*-MIG or an empty vector (EV) control. *BCR::ABL1* was used as a positive control known to confer cytokine-independent growth of Ba/F3 cells. In the absence of IL-3, expression of *CD74^{intr}::PDGFRB* was sufficient to drive cytokine independent proliferation similar to *BCR::ABL1* (Fig. 1d). Consistent with constitutive activation of PDGFRB, transformed *CD74^{intr}::PDGFRB⁺* Ba/F3 cells grown in the absence of IL-3 showed phosphorylation of PDGFRB (Y751) and Stat5 (Y694) that was blocked by treatment with imatinib (Fig. 1e). These findings were recapitulated in primary murine IL-7 dependent pre-B-cells transduced with *CD74^{intr}::PDGFRB* (Supplementary Fig. 1c).

¹Peter MacCallum Cancer Centre, Parkville, VIC, Australia. ²The Sir Peter MacCallum Department of Oncology, University of Melbourne, Parkville, VIC, Australia. ³Murdoch Children's Research Institute, Parkville, VIC, Australia. ⁴Walter and Eliza Hall Institute of Medical Research, Parkville, VIC, Australia. ⁵Department of Medical Biology, University of Melbourne, Parkville, VIC, Australia. ⁶Children's Cancer Institute, Lowy Cancer Research Centre, UNSW Sydney, Kensington, NSW, Australia. ⁷School of Clinical Medicine, UNSW Medicine & Health, UNSW Sydney, Sydney, NSW, Australia. ⁸Department of Paediatrics, University of Melbourne, Parkville, VIC, Australia. ⁹School of Biosciences, University of Melbourne, Parkville, VIC, Australia. ¹⁰School of Mathematics and Statistics, University of Melbourne, Parkville, VIC, Australia. ¹¹Children's Cancer Centre, Royal Children's Hospital, Parkville, VIC, Parkville, Australia. ¹²These authors contributed equally: Teresa Sadras, Fatimah B. Jalud. ✉email: paul.ekert@petermac.org

Received: 4 October 2022 Revised: 2 February 2023 Accepted: 6 February 2023
Published online: 21 February 2023

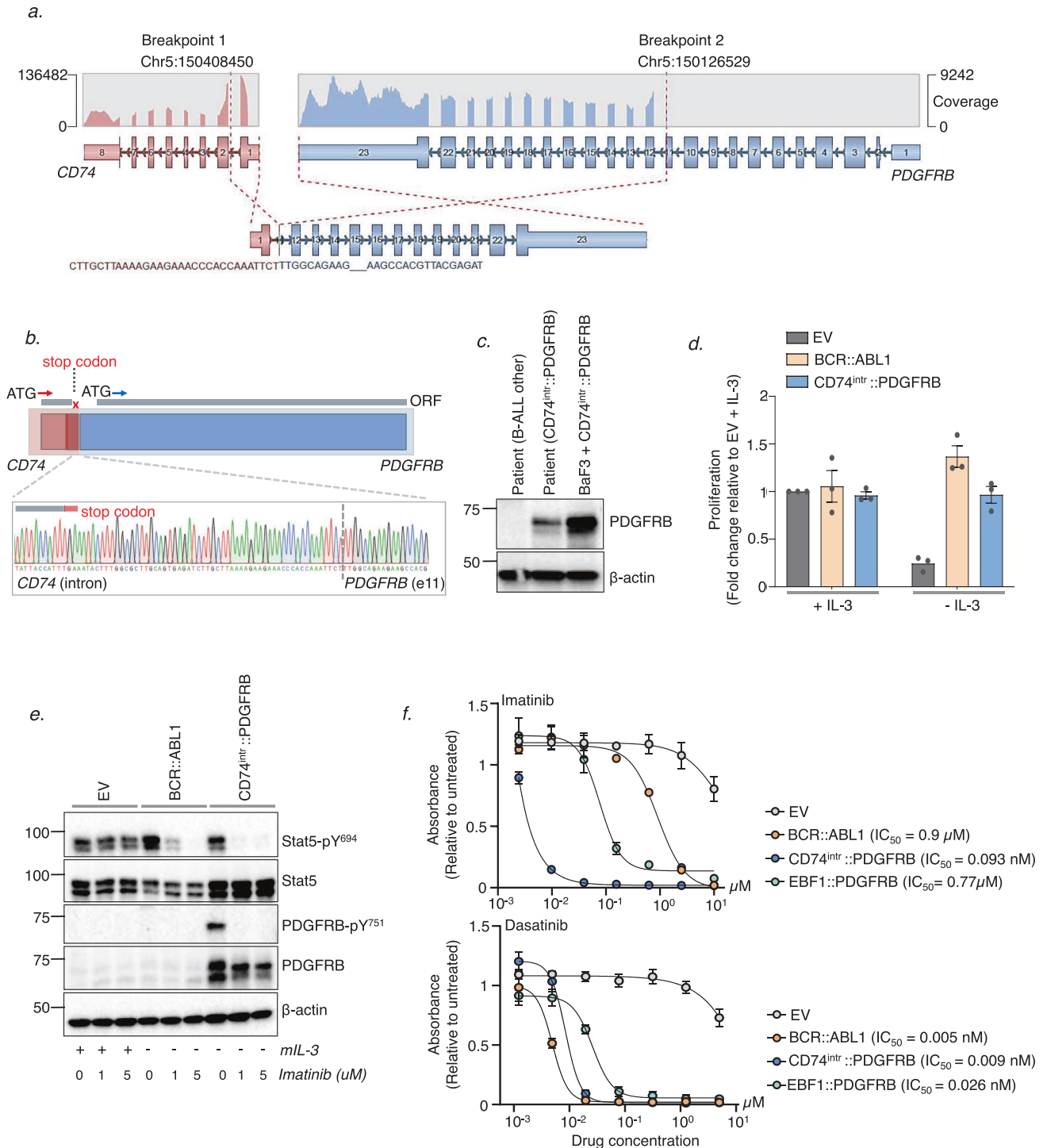
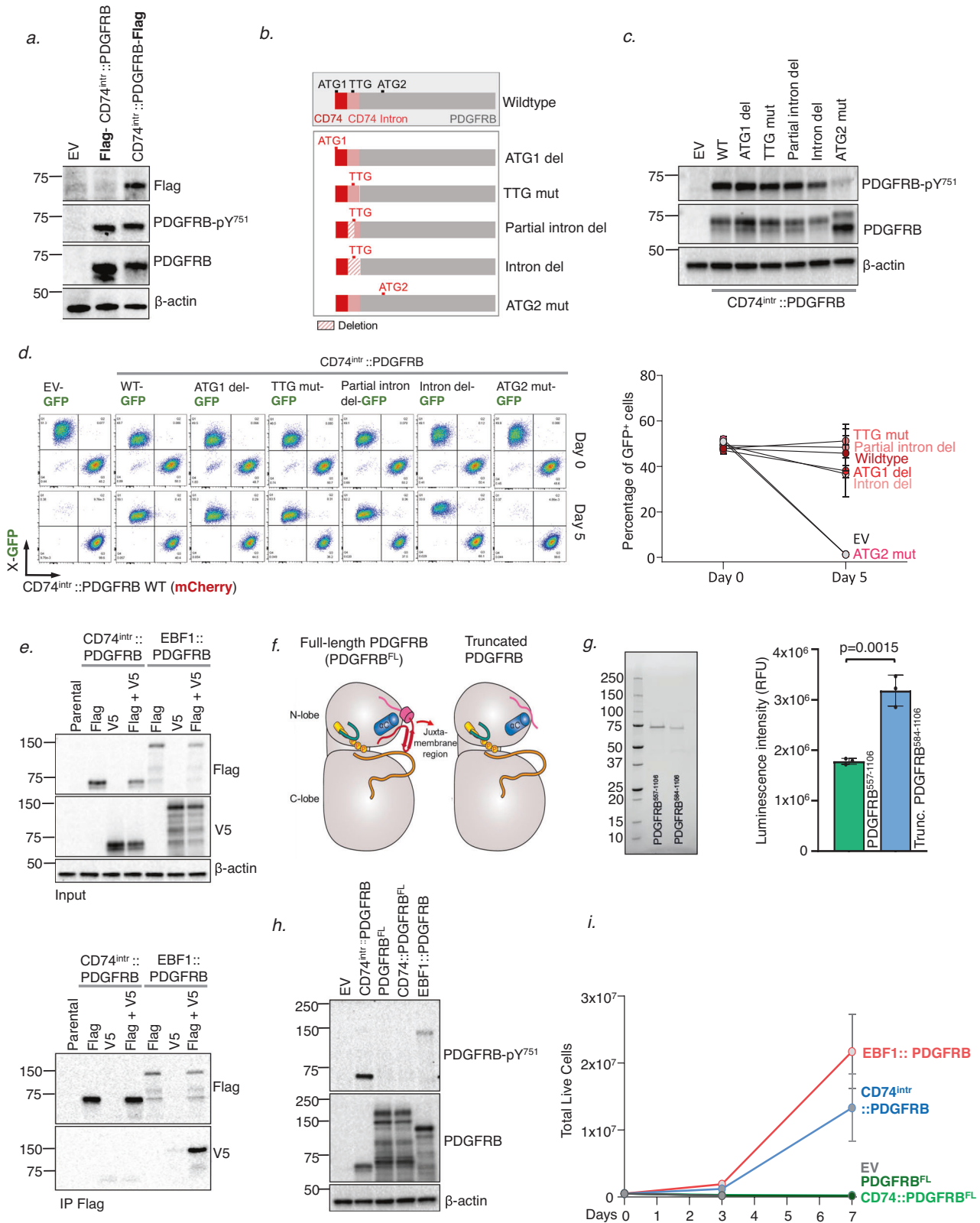


Fig. 1 Identification of atypical PDGFRB fusion in Ph-like B-ALL patient. **a** RNA-sequencing analysis identified a novel *CD74::PDGFRB* fusion between *CD74* (exon 1) and *PDGFRB* (exon 11) on chromosome 5. Image shown is modified from a fusion visualization tool Arriba [12]. RNA read coverage is shown across the genes involved in the fusion. **b** Sanger sequencing of the breakpoint shows a retained *CD74* intron sequence of 75 bp resulting in a stop codon before the fusion junction. A putative alternative open reading frame (ORF) starting at an ATG within *PDGFRB* exon 12 is also indicated. **c** Western blot analysis of PDGFRB in bone marrow MNCs from *CD74*^{intr}::*PDGFRB*⁺ patient. Ba/F3 cells expressing *CD74*^{intr}::*PDGFRB* and a second B-ALL patient with no known PDGFRB lesion were used as controls. **d** Proliferation of BCR::ABL1 and *CD74*^{intr}::*PDGFRB* expressing Ba/F3 cells following 48-hour IL-3 withdrawal. Proliferation was measured by luminescence relative to the EV control in IL-3 (day 0), using the CellTiter-Glo® 2.0 reagent. Data shows Mean ± SEM ($n = 3$). **e** Western blot analysis of BCR::ABL1 and *CD74*^{intr}::*PDGFRB* expressing Ba/F3 cells treated with 0, 1 or 5 μM imatinib for 6 hours. **f** Viability of BCR::ABL1, *CD74*^{intr}::*PDGFRB* and EBF1::*PDGFRB* expressing Ba/F3 cells treated with a dose titration of imatinib (top panel) or dasatinib (lower panel) for 72 hours, measured using the CellTiter-Glo® 2.0 reagent. Data is normalized to untreated cells. IC₅₀ values for each cell line is indicated. Data shows Mean ± SEM ($n = 3$).



Importantly, CD74^{intr}::PDGFRB-expressing Ba/F3 cells were highly sensitive to both imatinib and dasatinib in vitro (Fig. 1f).

Given the unusual structure of the CD74^{intr}::PDGFRB sequence, and the apparent lack of an ORF starting at the canonical ATG of CD74 exon 1, we investigated whether translation may be driven

by an alternate start site. For this, N- and C-terminal FLAG-tagged versions of CD74^{intr}::PDGFRB were expressed in Ba/F3 cells. While equivalent levels of p-PDGFRB (Y751) and total PDGFRB were detected in cells expressing the N- or C-terminal FLAG constructs (Fig. 2a), the FLAG epitope was only detected in cells expressing

Fig. 2 $CD74^{intr}::PDGFRB$ is driven by a non-canonical translation start site. **a** N- and C-terminal FLAG tagged $CD74^{intr}::PDGFRB$ constructs were transduced into Ba/F3 cells and analysed by Western blotting. **b** Schematic diagram of $CD74^{intr}::PDGFRB$ constructs with start codon mutations or deletions, and partial and full intron deletion. **c** Western blot analysis of $CD74^{intr}::PDGFRB$ mutants depicted in **b**, expressed in Ba/F3 cells. **d** Growth competition of Ba/F3 lines transduced with $CD74^{intr}::PDGFRB$ mutants. Ba/F3 lines expressing EV or $CD74^{intr}::PDGFRB$ constructs in GFP-expression plasmid, were mixed 1:1 with Ba/F3 cells expressing $CD74^{intr}::PDGFRB$ in mCherry-expression plasmid. GFP and mCherry populations were measured at day 0, and 5 days after mIL-3 withdrawal. Left panel shows representative FACS data, and right panel shows quantified GFP⁺ percentages (Mean \pm SEM) from 3 independent experiments. **e** FLAG-co-immunoprecipitation in HEK293T cells expressing FLAG or V5-tagged $CD74^{intr}::PDGFRB$ constructs, alone, or in combination. EBF1::PDGFRB was used as a positive control. Shown is whole cell lysate input (top panel) and western blot analysis of FLAG-immunoprecipitate elutes probed for FLAG or V5 (bottom panel). **f** AlphaFold2 structural modelling of full length PDGFRB (PDGFRB^{FL}) and $CD74^{intr}::PDGFRB$ highlighting loss of juxtamembrane region in $CD74^{intr}::PDGFRB$. **g** Left Panel: Reducing SDS-PAGE analysis of purified PDGFRB visualized by stain-free imaging to illustrate the purity of each PDGFRB preparation. Right Panel: In vitro kinase activities of PDGFRB⁵⁵⁷⁻¹¹⁰⁶ and truncated PDGFRB⁵⁸⁴⁻¹¹⁰⁶ encoded by the $CD74^{intr}::PDGFRB$ fusion. Individual data points are plotted; the bar and error bars shown represent mean \pm SD of three independent ADP-Glo assays. Presented data are representative of three technical replicates ($n = 9$). Statistical significance was calculated using an unpaired Student's *t* test. **h** Western blot analysis of Ba/F3 lines expressing PDGFRB variants. **i** Proliferation of Ba/F3 cells following withdrawal of IL-3 measured by trypan blue exclusion. Data shows Mean \pm SEM ($n = 3$). **h** Western blot analysis of Ba/F3 lines expressing PDGFRB variants. **i** Proliferation of Ba/F3 cells following withdrawal of IL-3 measured by trypan blue exclusion. Data shows mean \pm SEM ($n = 3$).

the C-terminal tag. This strongly suggests that translation of PDGFRB protein is not driven from the first ATG (ATG-1) within $CD74$. To validate this, and to more stringently dissect whether translation is driven from elsewhere within the $CD74$ -portion, we generated a construct with deletion of the ATG-1 codon from the $CD74^{intr}::PDGFRB$ sequence. We also sequentially deleted or mutated putative translation start sites within the $CD74^{intr}::PDGFRB$ fusion including a non-canonical TTG-codon within the retained $CD74$ -intronic region, and a putative ATG start site (ATG-2) in exon 12 of $PDGFRB$ (Fig. 2b). These constructs were expressed in Ba/F3 cells, and levels of p-PDGFRB (Y751) and PDGFRB were measured by western blotting (Fig. 2c). This revealed that only mutation of ATG-2 disrupted expression of an active protein. Strikingly, growth competition analyses of Ba/F3 lines expressing the $CD74^{intr}::PDGFRB$ mutants (in GFP expression plasmids), competing with WT $CD74^{intr}::PDGFRB$ (in mCherry expression plasmid) confirmed that mutation of ATG-2 abolished the transforming potential of the $CD74^{intr}::PDGFRB$ fusion (Fig. 2d).

Together, these results show that protein translation does not commence within $CD74$, and that the product from the $CD74^{intr}::PDGFRB$ fusion likely arises from an internal ATG within $PDGFRB$ itself, encoding a truncated PDGFRB molecule. In an analogous approach, we assessed the capacity for the $CD74$ -region to promote protein translation by generating an artificial hybrid construct of $CD74$ with the kinase domain of $ABL1$. This confirmed that the $CD74$ -sequence from $CD74^{intr}::PDGFRB$ is unlikely to drive translation of a fusion protein (Supplementary Fig. 1d).

Our findings provide evidence for a remarkable scenario, in which aberrant expression of a 'loose' PDGFRB kinase domain in B-cell progenitors is sufficient to drive auto-activation and leukemic transformation. This is particularly unique in the context of Ph-like ALL, which is characterized by expression of chimeric fusion proteins in which tyrosine kinase domains are fused in-frame to distinct N-terminal partners (commonly lymphoid transcription factors). Constitutive kinase activation of oncogenic chimeric-fusions is driven by retained oligomerization domains of N-terminal partner proteins, which mediate fusion homodimerization and subsequent auto-phosphorylation of the kinase domains. Notably, oligomerization domains of the partner proteins are indispensable for constitutive activation of other PDGFRB fusions (e.g. ETV6::PDGFRB and EBF1::PDGFRB [7]). Interestingly, co-immunoprecipitation (coIP) of FLAG-tagged $CD74^{intr}::PDGFRB$ in HEK293T cells suggests that unlike EBF1::PDGFRB, $CD74^{intr}::PDGFRB$ does not strongly dimerize (Fig. 2e). However, this does not exclude the possibility of a weak or transient dimerization driven instead by the stoichiometry of the abundance of the fusion. We note, for instance, that recombinant

truncated PDGFRB (PDGFRB⁵⁸⁴⁻¹¹⁰⁶) expressed and purified from insect cells elutes at a molecular weight consistent with a dimer (Supplementary Fig. 2a). Nonetheless, these findings suggest an alternative mechanism of activation for $CD74^{intr}::PDGFRB$ which may bypass the requirement for dimerization domains in the driver fusion.

To understand how a truncated PDGFRB kinase domain may be constitutively activated, we performed AlphaFold2 structural modelling comparing the intracellular portion of full-length (FL) human PDGFRB (PDGFRB^{FL}) and $CD74^{intr}::PDGFRB$ (Fig. 2f, Supplementary Fig. 2b). This revealed that the juxtamembrane (JM) domain partially occupies the ATP binding site by running parallel with the α C helix, before forming a β -strand hairpin that abuts the C-lobe of the kinase domain, occluding the active site. This is consistent with the experimental structure of the related protein, PDGFRA, where the active site is analogously occluded by the JM region [8]. In contrast, the truncated form of PDGFRB, encoded by the $CD74^{intr}::PDGFRB$ fusion, lacks the JM region and models predict that the active site is not obstructed in this setting. To test this hypothesis, we generated recombinant proteins to measure the kinase activity of PDGFRB⁵⁵⁷⁻¹¹⁰⁶ relative to the truncated form that arises from $CD74$ fusion, PDGFRB⁵⁸⁴⁻¹¹⁰⁶, in an ADP-Glo assay with a Poly-(Glu,Tyr) peptide substrate. While the replete intracellular portion of PDGFRB (PDGFRB⁵⁵⁷⁻¹¹⁰⁶) exhibited some catalytic activity, the truncated PDGFRB⁵⁸⁴⁻¹¹⁰⁶ protein displayed approximately double in vitro kinase activity (Fig. 2g).

Hence, we hypothesized, that unlike the 'truncated' $CD74^{intr}::PDGFRB$ protein, expression of the full-length PDGFRB (PDGFRB^{FL}) receptor may be ineffective in driving transformation as it is locked in an inactive state. To test this idea, we generated Ba/F3 lines expressing either the $CD74^{intr}::PDGFRB$ fusion or PDGFRB^{FL}. We also included a hybrid between $CD74$ and PDGFRB^{FL} ($CD74::PDGFRB^{FL}$), fusing the $CD74$ region to PDGFRB exon 1. Immunofluorescence staining revealed that both $CD74^{intr}::PDGFRB$ and PDGFRB^{FL} are dispersed through the cell cytoplasm (Supplementary Fig. 2c). Strikingly however, active PDGFRB protein (assessed by Y751 phosphorylation) was only observed in Ba/F3 cells expressing the $CD74^{intr}::PDGFRB$ construct, or EBF1::PDGFRB (Fig. 2h). Moreover, while Ba/F3 cells expressing $CD74^{intr}::PDGFRB$ proliferated in the absence of IL-3, cells expressing PDGFRB^{FL} or the $CD74::PDGFRB^{FL}$ hybrid did not (Fig. 2i, Supplementary Fig. 2d).

It remains to be determined whether there are other examples of cancer driven by a non-chimeric truncated PDGFRB protein or whether this mechanism of oncogenic activation extends to other kinases. Nonetheless, our observations are broadly relevant to oncogenic signaling given the recognized autoinhibitory function of the juxtamembrane domain in other type III receptor tyrosine kinases including PDGFRB/A [8, 9], c-KIT [10] and CSF1R [11].

Interestingly, molecular dissection of the *FIP1L1::PDGFRA* fusion, which occurs in chronic eosinophilic leukemia, demonstrated that FIP1L1 is entirely dispensable for PDGFRA activation, and that instead it is the partial loss of the JM domain within PDGFRA that drives constitutive activation of the fusion [9]. In the setting of PDGFR fusions which retain the intact JM domains (e.g. ETV6::PDGFRA [9], EBF1::PDGFRB [7]), autoinhibition is instead overcome by enforced dimerization driven by the N-terminal fusion partner, representing two distinct mechanisms by which PDGFR-family kinases may become constitutively activated in malignancy.

We present a unique example of aberrant expression of a non-chimeric 'loose kinase domain', which is targetable by ABL-class inhibitors (e.g. imatinib), driving Ph-like B-ALL. Our findings have critical implications for current pipelines of sequencing-based fusion identification, in which putative cancer drivers may be disregarded following out-of-frame predictions. This work also highlights the merit of functional validation of structurally unusual lesions, which may ultimately provide an invaluable opportunity for administration of targeted compounds in treatment regimens.

DATA AVAILABILITY

All data generated or analysed during this study are included in this published article and its Supplementary information files. Any other data may be requested from the corresponding author

REFERENCES

1. Roberts KG, Gu Z, Payne-Turner D, McCastlain K, Harvey RC, Chen IM, et al. High Frequency and Poor Outcome of Philadelphia Chromosome-Like Acute Lymphoblastic Leukemia in Adults. *J Clin Oncol*. 2017;35:394–401.
2. Den Boer ML, van Slegtenhorst M, De Menezes RX, Cheok MH, Buijs-Gladdines JG, Peters ST, et al. A subtype of childhood acute lymphoblastic leukaemia with poor treatment outcome: a genome-wide classification study. *Lancet Oncol*. 2009;10:125–34.
3. Mullighan CG, Su X, Zhang J, Radtke I, Phillips LA, Miller CB, et al. Deletion of IKZF1 and prognosis in acute lymphoblastic leukemia. *N. Engl J Med*. 2009;360:470–80.
4. Tran TH, Tasian SK. Has Ph-like ALL Superseded Ph+ ALL as the Least Favorable Subtype? *Best Pr Res Clin Haematol*. 2021;34:101331.
5. Schmidt B, Brown LM, Ryland GL, Lonsdale A, Kosasih HJ, Ludlow LE, et al. ALL-Sorts: an RNA-Seq subtype classifier for B-cell acute lymphoblastic leukemia. *Blood Adv*. 2022;6:4093–7.
6. Liu YF, Wang BY, Zhang WN, Huang JY, Li BS, Zhang M, et al. Genomic Profiling of Adult and Pediatric B-cell Acute Lymphoblastic Leukemia. *EBioMedicine*. 2016;8:173–83.
7. Welsh SJ, Churchman ML, Togni M, Mullighan CG, Hagman J. Deregulation of kinase signaling and lymphoid development in EBF1-PDGFRB ALL leukemogenesis. *Leukemia*. 2018;32:38–48.
8. Liang L, Yan XE, Yin Y, Yun CH. Structural and biochemical studies of the PDGFRA kinase domain. *Biochem Biophys Res Commun*. 2016;477:667–72.
9. Stover EH, Chen J, Folens C, Lee BH, Mentens N, Marynen P, et al. Activation of FIP1L1-PDGFRalpha requires disruption of the juxtamembrane domain of PDGFRalpha and is FIP1L1-independent. *Proc Natl Acad Sci USA*. 2006;103:8078–83.
10. Chan PM, Ilangumaran S, La Rose J, Chakrabarty A, Rottapel R. Autoinhibition of the kit receptor tyrosine kinase by the cytosolic juxtamembrane region. *Mol Cell Biol*. 2003;23:3067–78.
11. Walter M, Lucet IS, Patel O, Broughton SE, Bamert R, Williams NK, et al. The 2.7 Å crystal structure of the autoinhibited human c-Fms kinase domain. *J Mol Biol*. 2007;367:839–47.
12. Uhrig S, Ellermann J, Walther T, Burkhardt P, Frohlich M, Hutter B, et al. Accurate and efficient detection of gene fusions from RNA sequencing data. *Genome Res*. 2021;31:448–60.

ACKNOWLEDGEMENTS

We gratefully acknowledge the Research Genomics Facility of the Victorian Clinical Genetics Service. Tumour samples and coded data were supplied by the Children's Cancer Centre Biobank at the Murdoch Children's Research Institute and The Royal Children's Hospital (mcri.edu.au/research/projects/childrens-cancer-centre-biobank). Establishment and running of the Children's Cancer Centre is made possible through generous support by Cancer In Kids @ RCH (www.cika.org.au), The Royal Children's Hospital Foundation and the Murdoch Children's Research Institute and the Children's Cancer Centre Tissue Bank (Murdoch Children's Research Institute). This work is supported by National Health and Medical Research Council Grants (1140626 to P.G.E.; 1172929 and 9000719 to JMM) and a SCOR Grant (7015-18) from the Lymphoma and Leukemia Society. We acknowledge the support of Perpetual Trustees and the Samuel Nissen Foundation. S.L.K. is supported by a fellowship from the Victorian Cancer Agency. This work was also supported by the Victorian Government's Operational Infrastructure Support Program.

AUTHOR CONTRIBUTIONS

TS, FBJ, HJK, CRH, and LMB contributed to the design, conduct and analysis of experimental data presented in this manuscript. CRH and JMM designed performed and analyzed the experiments with recombinant proteins and generated the alpha-fold models. SE-K, MJC, NMD and AO analysed structural features of the fusion gene and contributed to the design of mutational experiments. LEAL, and SLK contribute to the identification of eligible samples, the collation and presentation of clinical data. TS, AO, JMM, CEdeB, APN, NMD, contributed to the concept and design of experiments and the analysis of experimental data. TS and PGE conceived and designed the project and wrote the manuscript. All authors contributed to the revision of manuscript drafts.

FUNDING

Open Access funding enabled and organized by CAUL and its Member Institutions.

COMPETING INTERESTS

PGE, JMM, SLK and APN receive an annual payment related to the Walter and Eliza Hall Institute distribution of royalties scheme. PGE consults for Illumina.

ADDITIONAL INFORMATION

Supplementary information The online version contains supplementary material available at <https://doi.org/10.1038/s41375-023-01843-x>.

Correspondence and requests for materials should be addressed to Paul G. Ekert.

Reprints and permission information is available at <http://www.nature.com/reprints>

Publisher's note Springer Nature remains neutral with regard to jurisdictional claims in published maps and institutional affiliations.



Open Access This article is licensed under a Creative Commons Attribution 4.0 International License, which permits use, sharing, adaptation, distribution and reproduction in any medium or format, as long as you give appropriate credit to the original author(s) and the source, provide a link to the Creative Commons license, and indicate if changes were made. The images or other third party material in this article are included in the article's Creative Commons license, unless indicated otherwise in a credit line to the material. If material is not included in the article's Creative Commons license and your intended use is not permitted by statutory regulation or exceeds the permitted use, you will need to obtain permission directly from the copyright holder. To view a copy of this license, visit <http://creativecommons.org/licenses/by/4.0/>.

© The Author(s) 2023